

ZDRAVKA K. DJUMAILIEVA<sup>1</sup>, DIMKA I. FACHIKOVA<sup>1\*</sup>, GERGANA P. ILIEVA<sup>1</sup>,  
TSVETELINA L. LIUBENOVA<sup>1</sup>

## KINETICS AND CHARACTERIZATION OF PHOSPHATE COATINGS PREPARED ON ALUMINUM SURFACES

The electrochemical formation of phosphate thin coatings on aluminum alloy AA1050 has been studied. The mass/thicknesses of the films were determined by gravimetric measurements at different conditions: concentration of the working solutions 2.0-11.0 vol.%; duration of the processes 1.0-10.0 min; temperature in the range of 20.0-70.0°C; cathodic current densities 0.1-0.5 Adm<sup>-2</sup>. The chemical elements containing in the phosphate coatings were determined by EDX-analysis. The morphology and topography of the coatings were studied by SEM. The corrosion behavior and the protective ability of the phosphate coatings are investigated by potentiodynamic polarization method (PDPM) and by electrochemical impedance spectroscopy (EIS). It has been found that as the concentration, temperature and density of the polarizing cathode current density rises, the mass of the phosphate films increases – the thinner ones being dense and uniform, while the thicker ones are cracked. Mainly phosphorus, oxygen, molybdenum and nickel exist in the coatings and their amounts increase with temperature of the phosphating bath is raised while the Al content in the coatings reduces at the same conditions. The corrosion of the phosphated specimens increase slightly with a rise in the temperature of the solutions during their phosphating, when the cracks in the coatings and resp. the bare metal of the substrate increases. The uncoated specimen has lower barrier ability, while the phosphated has higher barrier ability in the corrosion medium.

*Keywords:* Aluminum alloys; conversion coatings; phosphating; tin films; corrosion

### 1. Introduction

Aluminum and its alloys, because of their good mechanical, technological, electrical, thermal, corrosion-resistant properties, are increasingly used in various sectors of industry. Because of the highly negative electrode potential, aluminum and many of its alloys are unstable in many natural and industrial corrosive environments, especially in contact with noble metals. To improve their corrosion resistance, as well as to improve the adhesion of subsequently applied organic coatings, the pretreatments of aluminum surfaces are highly recommended [1-5].

Chemical conversion coatings are the most widely used pretreatment process for aluminum substrates. These include anodizing, chromating, accelerated chromate phosphates, chromate oxides [6-8], and recently nonchromating formulations reported [9-16,21-23]. Historically, however, phosphoric acid cleaners, wash primers, crystal, and amorphous phosphates have been utilized as paint pretreatments with satisfactory results. The amorphous phosphate coatings should be mentioned as promising treatments [17-19].

This paper presents the results obtained when studying the influence of different factors (concentration and temperature of working solutions; duration of processes; cathodic current density) on the kinetics of formation of thin phosphate films on aluminum surfaces, as well as their characterization by EDX, SEM, PDPM and EIS analyses.

### 2. Experiment

#### 2.1. Material and samples

The samples for the kinetics studies were made from aluminum alloy AA1050, with a rectangular shape (thickness 0.5 mm and working surface  $1 \times 10^{-3} \text{ m}^2$ ) (see TABLE 1 – the chemical composition was taken from the certificate of the material purchased). Electrochemical experiments are carried out with plate-shaped specimens with a fixed working area of  $0.02 \text{ dm}^2$ . In addition, for the physics-analytical methods, disk-shaped specimens ( $1 \times 10^{-3} \text{ m}^2$ ) were used in the presented work.

<sup>1</sup> UNIVERSITY OF CHEMICAL TECHNOLOGY AND METALLURGY, FACULTY OF CHEMICAL TECHNOLOGY, 8 KLIMENT OHRIDSKI BLVD., 1756 SOFIA, BULGARIA

\* Corresponding author: [dimkaivanova@uctm.edu](mailto:dimkaivanova@uctm.edu)



Chemical composition of aluminum alloy AA 1050 (% in mass)

Al	Cu	Fe	Mg	Mn	Si	Ti	V	Zn
99.5	0.05	0.4	0.05	0.05	0.25	0.03	0.05	0.05

## 2.2. Solutions

The phosphating liquid concentrate contains ammonium and sodium orthophosphates, molybdates, and phosphoric acid. Also, softeners, inorganic activators, as well as surfactants, stabilizing agents, and accelerators are added.

The working media are aqueous solutions of the phosphating concentrate with concentrations in the range of 2.0-11.0 vol.%. The experiments are carried out in a temperature range 20.0-70°C and a process duration 1.0-10.0 min. The working/model media used for corrosion experiments is 0.01 M NaCl.

## 2.3. Methods

### 2.3.1. Gravimetric method

The gravimetric method was used to study the kinetics of forming and determining the process conditions for the phosphate coating's mass/thickness growth, depending on the influence of different factors. The method allows determining a mass/thickness alteration of specimens after forming and removing the coatings:

$$M = \frac{m_1 - m_2}{S}, \text{ gm}^{-2}$$

where:  $M$ ,  $\text{gm}^{-2}$  is the mass (or accepted to call a thickness) of the obtained coating,  $m_1$  and  $m_2$  are respectively the sample mass after forming and after removal of the coating, g;  $S$  is the sample surface area,  $\text{m}^2$ .

### 2.3.2. Electrochemical methods

Electrochemical measurements were performed in a three-electrode electrochemical cell, which combines a galvanic cell between the working and reference electrodes and an electrolysis cell, between the working and counter electrodes (Fig. 1) [20].

*Potentiodynamic polarization method.* The polarization curves recorded potentiostatically or potentiodynamically allow the determination of various electrochemical and corrosion characteristics such as a corrosion rate, a corrosion potential, etc. All electrochemical measurements were performed in a model 0.01 M NaCl solution in the range of potentials from  $-0.060$  to  $+600$  mV (vs. OCP) and a scan rate of the potential  $5 \text{ mV s}^{-1}$ .

*Electrochemical impedance spectroscopy (EIS).* Measurements were performed in standard three-electrode "flat" cells (ISO 16773-2), fitted with a platinum mesh as the opposite electrode and Ag/AgCl-3M KCl as a reference electrode. EIS

spectra were recorded in the frequency range of 10 kHz to 0.01 Hz, distributed in 50 measuring points. The amplitude of the excitation signal was set by 10 to 35 mV, regarding the open circuit potential (OCP), to obtain spectra without scattering the measured points.

The instrument for electrochemical methods is an AUTO-LAB-30 Potentiostat/Galvanostat, using a specialized software product "General Purpose Electrochemical System" from Metrohm (Netherlands), equipped with an FRA-2 frequency analyzer (for EIS).

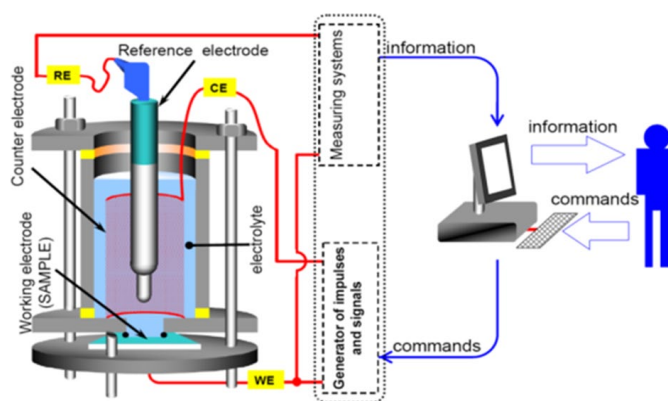


Fig. 1. Schematic diagram of the equipment used

### 2.3.3. Physical methods

*Scanning electron microscopy (SEM).* The morphology and structure of the coatings were examined by scanning electron microscopy, using a SEM/FIB LYRA I XMU, TESCAN electron microscope, equipped with ultrahigh-resolution scanning system secondary electron image (SEI). The SEM apparatus has the following characteristics: electronic source – tungsten heater, resolution – 3.5 nm at 30 kV.

*Energy dispersive X-ray spectroscopy (EDX).* The energy dispersive spectroscopy is a local X-ray spectral analysis that permits qualitative and quantitative determination of surface micro-volume contents of the order of several  $\mu\text{m}^3$ . Apparatus Quantax 200, BRUKER with spectroscopic resolution at Mn-K $\alpha$  and 1 kcps 126 eV is used. The accelerating voltage of the X-ray beam is 20 kV.

## 3. Results and discussion

### 3.1. Gravimetric measurements

The mass/thickness growth of the thin phosphate films on AA 1050 aluminum alloy samples was determined by gravimetric

measurements before and after film formation, taken per unit area of the treated surface, respectively. The removal of the film was carried out in boiling solutions of chromium anhydride and phosphoric acid for about a minute. Four series of experiments were carried out, depending on the concentration of the phosphating solution. The effect of cathodic polarization (0.1; 0.3; 0.5  $\text{Adm}^{-2}$ ) on the mass/thickness of the thin phosphate films in solutions with a concentration of 2.0 vol.% and temperatures 20.0, 30.0, 40.0, 50.0, 60.0 and 70.0°C, (denoted as series 1) is illustrated in Fig. 2. From the course of curves, it is seen that the mass/thickness of the phosphate films increases with time and the polarizing cathode current density for the temperature range studied. The mass/thickness of the films developed in solutions of 70.0°C is about twice that formed in solutions at lower temperatures (20.0 and 30.0°C).

The coatings (series 1) are mostly light in color and range from light grey and light blue, pale yellow and light green to pale brown. There is a tendency for color compaction with increasing sample processing time and cathodic current density.

The effect of the cathodic polarization on the mass/thickness of thin phosphate films – series 2 (in a solution of 4 vol.% and temperatures 20.0, 30.0, 40.0, 50.0, 60.0 and 70.0°C) is shown in Fig. 3. The graphs show that the increase of the coating's mass/thickness is like that for series 1 (with an increase in

processing time or a cathode current density), but the coatings (series 2) are 1.5-2 times thicker. However, upon the conditions imposed at the lower temperatures of the solution (20.0 and 30.0°C) the average mass/thicknesses of the films are comparable to the ones obtained with the samples in series 1 obtained at 50.0 and 60.0°C.

Moreover, the films (series 2) obtained at the higher working temperatures (60.0 and 70.0°C), are about twice thicker than the ones formed at lower temperatures of the phosphating baths (20.0 and 30.0°C).

The colors of the coatings (series 2) are in general light and vary from pale-yellow, blue-purple, and light green to dark brown. Here again, there is a tendency for the colors to be darker with the increase in both the treatment time and current density.

The results for the samples in series 3 showing the effect of the cathodic polarization (in solutions with 7 vol.% and temperatures 20.0, 30.0, 40.0, 50.0, 60.0 and 70.0°C) reveal that the mass/thickness growth is almost linear with increases in both temperature and the current density, thus confirming the tendency established with the samples in series 1 and 2 (see Fig. 4). The maximum was observed with films developed in 60.0 and 70.0°C baths, and was about twice that obtained in series 2 under the same operating conditions. The thicknesses obtained in such high-temperature baths are very similar, and therefore

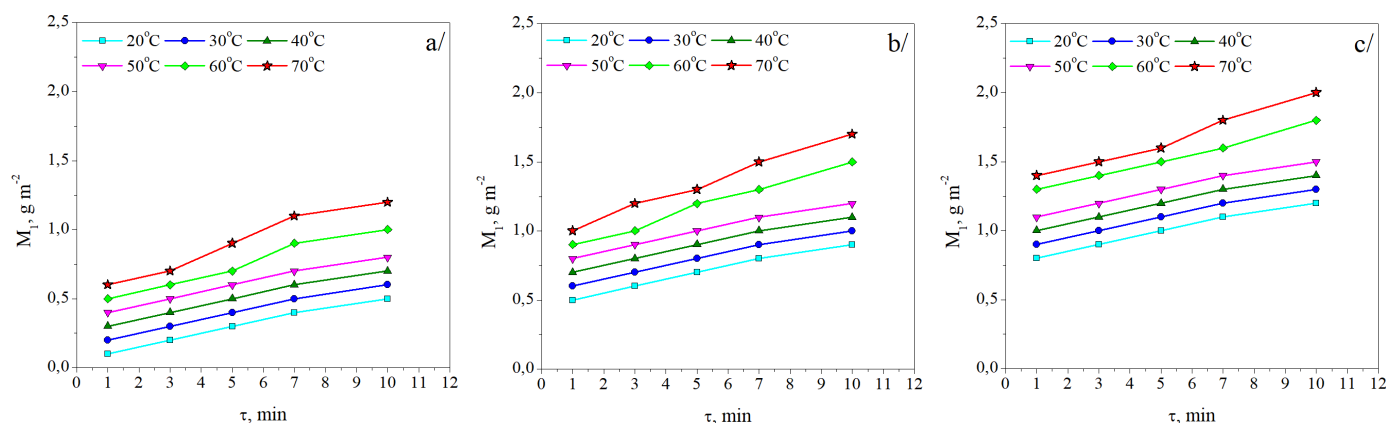


Fig. 2. Mass/thickness film growth in time, " $m_1, \text{gm}^{-2} - \tau, \text{min}$ ", for samples treated in 2.0 vol.% solutions at various temperatures and three cases of current density: (a) 0.1  $\text{Adm}^{-2}$ ; (b) 0.3  $\text{Adm}^{-2}$ ; (c) 0.5  $\text{Adm}^{-2}$

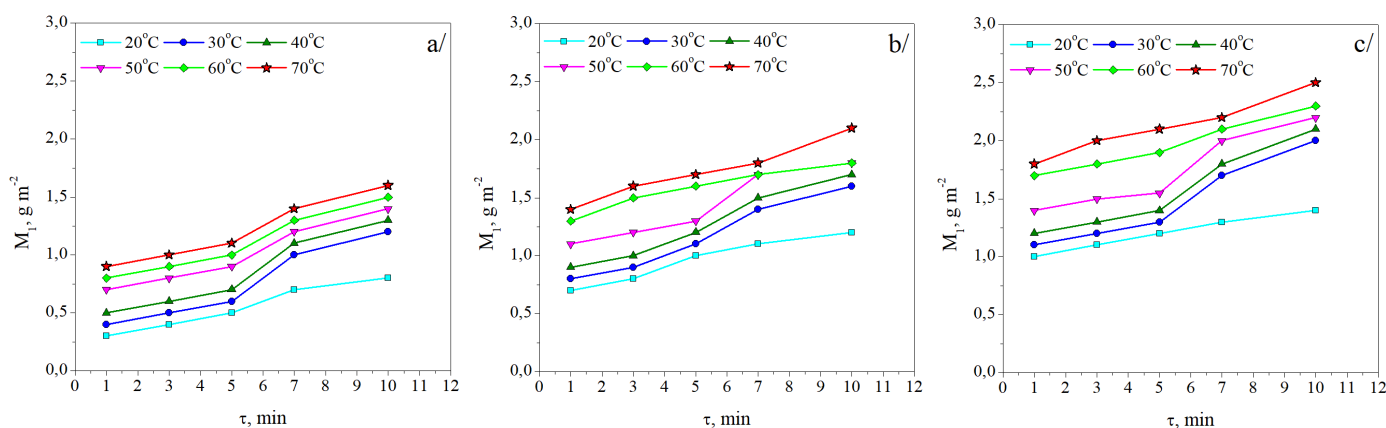


Fig. 3. Mass/thickness film growth in time, " $m_1, \text{gm}^{-2} - \tau, \text{min}$ ", for samples treated in 4.0 vol.% solutions at various temperatures and three cases of current density: (a) 0.1  $\text{Adm}^{-2}$ ; (b) 0.3  $\text{Adm}^{-2}$ ; (c) 0.5  $\text{Adm}^{-2}$

from a practical point of view it would be more reasonable to carry out the process in low-temperature baths.

The colors of the coating obtained in series 3 are brighter and vary from blue, yellow, and orange when low-temperature baths are used and from green, dark purple, and black in high-temperature solutions.

For the cases corresponding to series 4, the effect of the cathodic polarization on the mass/thickness of the phosphating conversion coatings is a slight (obtained in baths with 11.0 vol.% and temperatures 20.0, 30.0, 40.0, 50.0, 60.0, and 70.0°C) when high-temperature baths are applied (see Fig. 5). This could be attributed to the initial stages in both the nucleation process and consequent growth of the coatings that occur with high rates (at upon high concentration conditions), higher than in the series with lower concentrations. Such rapid initial nucleation and growth rates reduce subsequent film growth because the surface is already covered, and the initial layers make mass transfer difficult.

The colors of the coatings obtained in Series 4 samples have similar nuances to series 3 coatings but are generally darker. At higher temperatures, the dominant coatings are mostly dark brown or black.

In general, thin phosphate coatings, independent of the experimental series, have colors highly dependent on tempera-

ture and exposure time at a given cathodic polarization value. The colors become darker as the temperature of the solutions increases.

### 3.2. SEM analysis

Microphotographs of phosphate films on the aluminum alloy AA 1050 are shown in Fig. 6 – per given temperature, lasting time 5 minutes, 7.0 vol.% and a current density of  $0.1 \text{ Adm}^{-2}$ . At all conditions of the coating's developments, the sample surfaces are covered almost homogeneously with dense fine films and the reproducibility of the process is satisfactory high. The analysis was carried out with samples taken from each series.

At bath temperatures of 20.0 and 30.0°C (Figs. 6a and 6b), the coatings have homogeneous and uniform surfaces. At average temperatures (Figs. 6c and 6d), grooving/cracking coatings and formation of individual plates with different geometric shapes appear (in the bath at 50.0°C, the shape of the individual plates is mostly rectangular). The coatings obtained at high temperatures (Figs. 6e and 6f) have highly cracked structures and the plates are separated from each other by wide grooves ranging from 1 to  $2 \mu\text{m}$  for the coating obtained at 60.0°C and from 2 to  $12 \mu\text{m}$  for the films developed at 70.0°C. For the chromate and phosphate

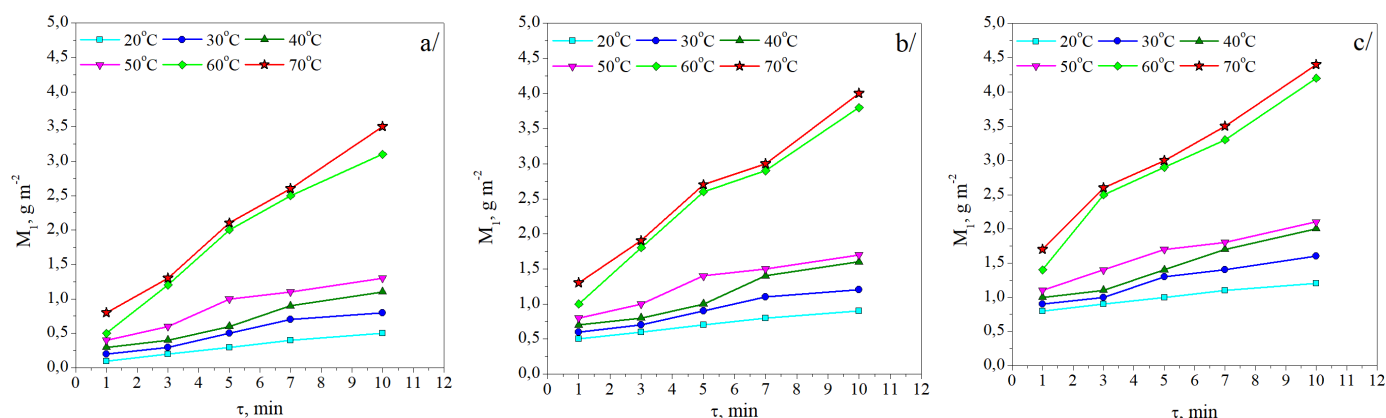


Fig. 4. Mass/thickness film growth in time, " $m_1, \text{gm}^{-2} - \tau, \text{min}$ ", for samples treated in 7.0 vol. % solutions at various temperatures and three cases of current density: (a)  $0.1 \text{ Adm}^{-2}$ ; (b)  $0.3 \text{ Adm}^{-2}$ ; (c)  $0.5 \text{ Adm}^{-2}$

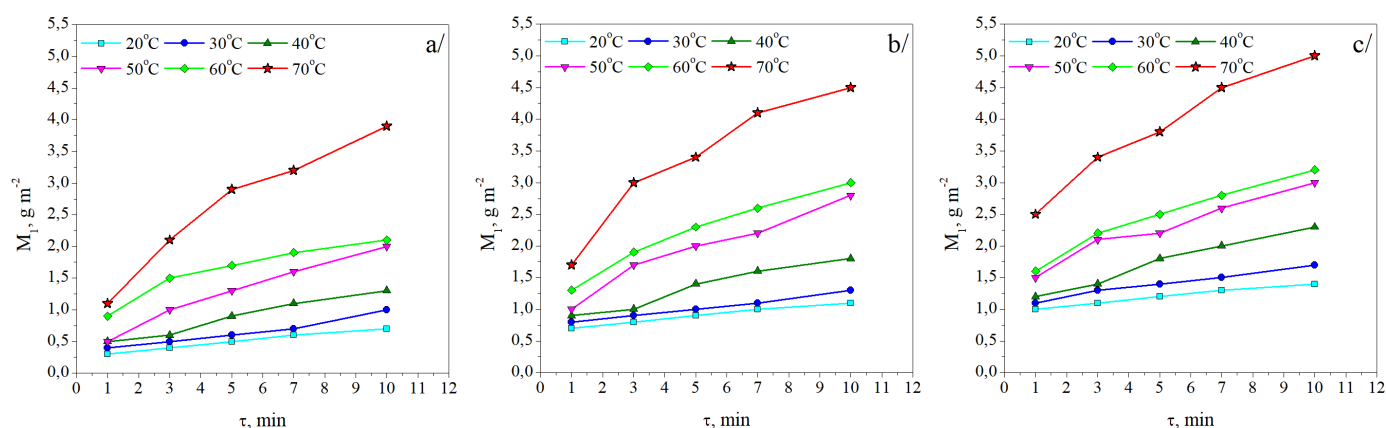


Fig. 5. Mass/thickness film growth in time, " $m_1, \text{gm}^{-2} - \tau, \text{min}$ " for samples treated in 11.0 vol.% solutions at various temperatures and three cases of current density: (a)  $0.1 \text{ Adm}^{-2}$ ; (b)  $0.3 \text{ Adm}^{-2}$ ; (c)  $0.5 \text{ Adm}^{-2}$



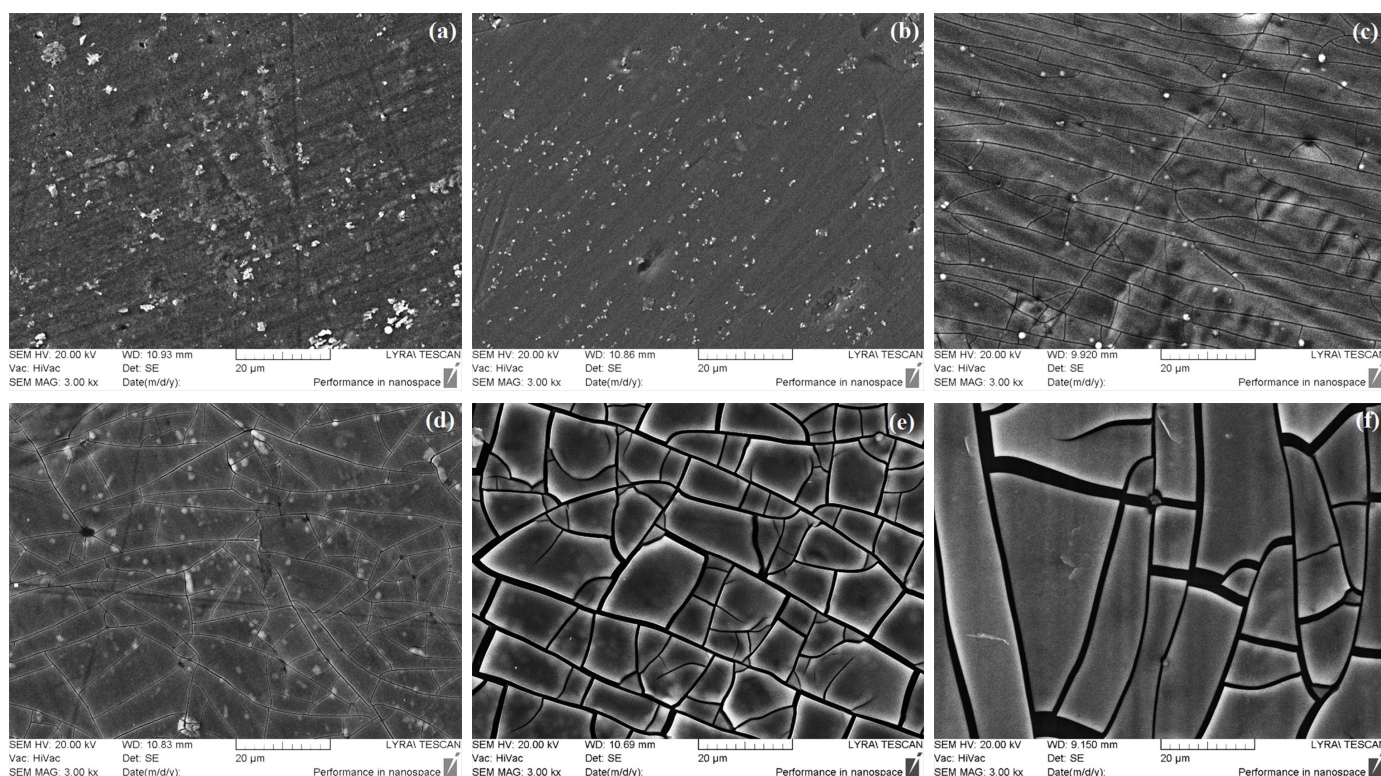


Fig. 6. Microphotographs of thin phosphate coatings obtained in baths of various temperatures: (a) 20.0°C; (b) 30.0°C; (c) 40.0°C; (d) 50.0°C; (e) 60.0°C; (f) 70.0°C

conversion coatings this effect is well-known in the literature as “dry riverbed”. It would be expected that the surfaces with more grooves would assure stronger adhesion of the polymeric coatings, for instance.

### 3.3. EDS analysis

The main elements found in the coatings are summarized in TABLE 2 – for a given temperature, a process lasting 5 minutes, a concentration 7.0 vol.% and a current density of  $0.1 \text{ A dm}^{-2}$ . The data revealed that the amounts of O, P and Mo increased with raise bath temperature and the greater content corresponded to the samples treated at 70°C. At the same time, there is a decrease in aluminum in phosphate films, with an increase in their thickness.

TABLE 2

Elemental contents of conversion phosphate coatings obtained upon various experimental conditions – 20.0÷70.0°C, 5 min, 7.0 vol.% and  $0.1 \text{ A dm}^{-2}$  [At.%]

Elements	20.0°C	30.0°C	40.0°C	50.0°C	60.0°C	70.0°C
	At.%	At.%	At.%	At.%	At.%	At.%
Al	79.55	74.60	52.57	49.93	30.96	21.67
O	17.91	22.16	40.53	42.20	52.54	62.51
Na	1.36	1.33	1.29	1.65	2.93	2.31
Mo	0.59	0.94	3.04	3.18	6.99	7.73
P	0.51	0.86	2.36	2.61	5.85	5.23
Ni	0.09	0.10	0.20	0.43	0.73	0.55
Total:	100	100	100	100	100	100

### 3.4. Polarization measurements

Polarization measurements were performed with six phosphate coated samples. The coatings were formed at different temperatures (20.0–70.0°C) in 7.0 vol.% solutions, for 5 minutes and a current density of  $0.1 \text{ A dm}^{-2}$ . The conditions were selected from the gravimetric studies, considering the reproducibility and mass/thickness of the obtained coatings. All measurements were carried out in a corrosion environment – 0.01 M NaCl.

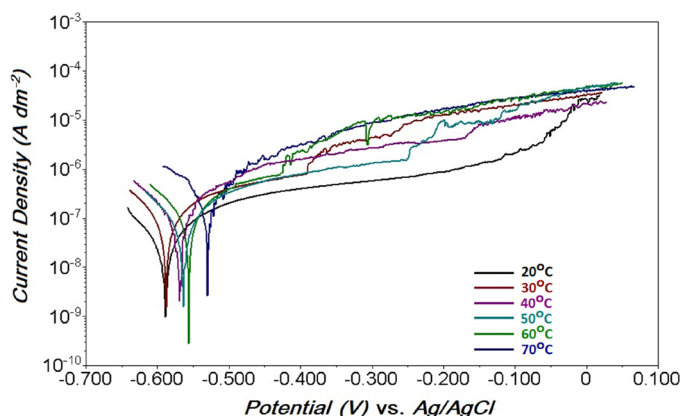


Fig. 7. Potentiodynamic polarization relationships of phosphated specimens taken at room temperature in 0.01 M NaCl, in the range of potentials from -0.060 to +600 mV (vs. OCP) and a potential scan rate  $5 \text{ mV s}^{-1}$

From the polarization relationships “Potential, V (vs. Ag/AgCl) – Current Density,  $\text{A dm}^{-2}$ ”, presented in Fig. 7, it can

be seen that there is no significant difference in the course of the curves. In the anode part of the relationships, a fluctuation of the potentials is observed, the beginning of which shifts to more negative values for the samples phosphated at higher temperatures.

The parameters *Open circuit potential* (OCP)  $E$ , V, *Corrosion potential*  $E_{corr}$ , V and *Polarization resistance*  $R_p$ ,  $\Omega \cdot \text{cm}^2$  – TABLE 3, were determined from the polarization relationships. The shift of  $E$ , V (OCP) and  $E_{corr}$ , V to more positive values, although slightly – around 0.050 V, can be explained by the larger mass/thickness of the phosphate films obtained at higher temperatures. The difference of the *Open circuit potential*  $E$ , mV (OCP) and the *Corrosion potential*  $E_{corr}$ , mV, can be attributed to the fact that the former was recorded automatically by the measuring device, while the second one was determined via analysis of the polarization curves, precisely after the plotting of its cathodic branch.

TABLE 3

Data corresponding to the polarization curves (see Fig. 7)

Sample	$E$ , V (OCP)	$E_{corr}$ , V	$R_p$ , $\Omega \cdot \text{cm}^2$
20°C	-0.582	-0.589	192.70
30°C	-0.579	-0.588	178.80
40°C	-0.572	-0.569	163.60
50°C	-0.557	-0.563	151.10
60°C	-0.551	-0.556	142.60
70°C	-0.533	-0.530	129.05
Average value	-0.558	-0.566	159.64

An inverse-proportional dependence is known to exist between polarization resistance,  $R_p$  and corrosion current,  $I_{corr}$ . The more value  $R_p$  has, the smaller  $I_{corr}$  is – that is, at a smaller rate corrodes the coating/metal. From the  $R_p$  values in TABLE 3, it follows that the corrosion of the test specimens increases with a raising in the temperature of the solutions during their phosphating, when the cracks in the coatings, resp. and the bare metal area of the substrate increase.

The impedance spectra of the tested samples shown in Fig. 8 reveal that results for the uncoated sample of AA 1050 (1) and the coated in a 7.0 vol.% solution, for 5 minutes at 70°C and a current density of  $0.1 \text{ A dm}^{-2}$  sample (2), differ substantially – the coated sample has a higher barrier ability, respectively higher corrosion resistance. The corrosion behaviour of phosphate coatings can be explained based on a porous film model, since the interface (corrosion solution/coating-metal) approximates such a model. This implies that the metal substrate is corroding in the same way where coverage is lacking – in a much smaller area. Since the capacitive and resistive contributions vary directly and indirectly, respectively, with respect to the area, based on these measured parameters, predictions on the corrosion rate of different phosphate coatings can be easily made.

The most suitable model electrical equivalent circuit for analyzing the impedance spectra is presented in Fig. 9.

The comparison of the impedance spectra can be carried out in a better way through the numerical values summarized

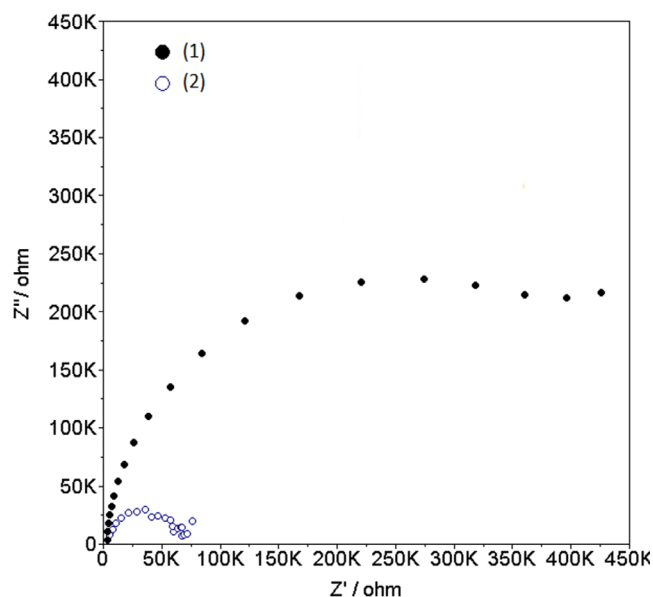


Fig. 8. Electrochemical impedance spectra (Nyquist) of uncoated (1) and phosphated (2) specimen after immersion in a corrosive (0.01 M NaCl) medium

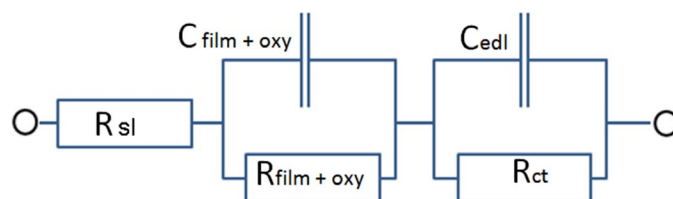


Fig. 9. Equivalent electrical circuit corresponding to the impedance at the interface between the specimen and the electrolyte:  $R_{sl}$  – ohmic resistance of the solution;  $R_{film}$  – ohmic resistance of the coatings;  $C_{film}$  – capacitance of the phosphating coating

in TABLE 4. The uncoated sample shows a lower resistance and a higher capacitance, which is attributed to the lower barrier ability.

TABLE 4

Parameters of the equivalent electric circuit corresponding to the impedance spectra of tested coated samples

Samples	$R_{sl}$ , $\Omega \text{ cm}^2$	$C_{film}$ , $\mu\text{F cm}^{-2}$	$R_{film}$ , $\text{k}\Omega \text{ cm}^2$
Uncoated Al sample	$581.00 \pm 10.41$	$114.85 \pm 17.2$	$60.48 \pm 1.72$
Sample 70°C	$495.00 \pm 12.13$	$15.95 \pm 1.21$	$157.78 \pm 19.07$

#### 4. Conclusions

The proposed work presents the results obtained in the complex study of the electrochemical formation processes of thin phosphate coatings on aluminum alloy AA1050. The values of the parameters governing the phosphating processes – concentration, temperature, duration, cathodic polarization, etc. have been studied and optimized. The mass/thickness, the chemical content and the morphology of phosphate films, formed in solu-

tions containing ammonium and sodium phosphates, molybdates, softeners, inorganic activators, buffers and surfactants, have been determined by applying gravimetric, X-Ray, microscopic and electrochemical methods. The main results can be outlined as:

1. The mass/thickness of the coatings rises with an increase of the solution concentration (2.0-11.0 vol.%), bath temperature (20.0-70.0°C), and the density of the cathodic polarization current (0.1-0.5  $\text{Adm}^{-2}$ ), for all cases presented in this report.
2. The SEM – analysis shows that the thinner coatings are dense and fine (Figs. 6a, 6b), while in the thicker coatings grooves and cracks appear (Figs. 6c-6f).
3. The elemental analysis of the coatings indicates that mainly phosphorus, oxygen, molybdenum and nickel exist in them. The amounts of O, P, Ni and Mo increase when the temperature of the phosphating bath is raised. The Al content in the coatings reduces with an increase of their mass/thickness.
4. The potentiodynamic polarization measurements of the phosphated specimens taken in 0.01 M NaCl showed that the corrosion potential, although slightly, shifted to more positive values, and the corrosion current to higher values, with an increase in the temperature of the phosphating solutions in which the coatings are obtained: it follows that the corrosion of the test specimens increase slightly with a raising in the temperature of the solutions during their phosphating, when the cracks in the coatings, resp. and the bare metal area of the substrate increase.
5. The analysis of the impedance spectra reveals that the uncoated sample has lower barrier ability, while the coated sample has higher barrier ability in a corrosive medium.

Conversion phosphate coatings are very rarely used alone, most often they serve as a basis for organic coatings, because significantly increase their adhesion to the metal-substrate. As a continuation of the presented work, the influence of the type, the method of application (mechanical, immersion, electrostatic, etc.) and the intended use on the adhesion, strength, UV, bio, corrosion resistance and protective ability of different organic coatings applied to aluminum surfaces treated in the work-studied phosphating solutions and conditions will be studied.

#### Acknowledgments

This work is developed as part of contract №: BG-RRP-2.004-0002-C01, project name: BiOrgaMCT, Procedure BG-RRP-2.004 “Establishing of a network of research higher education institutions in Bulgaria”, funded by Bulgarian National Recovery and Resilience Plan.

#### REFERENCE

[1] S. Wernic, R. Pinner, Surface treatment and finishing of aluminum and its alloys, Teddington (Middlesex, England): Robert Deaper, 1996.

[2] P.G. Sheasby, R. Pinner, The surface treatment and finishing of aluminum and its alloys, sixth edition, Redwood Books, Trowbridge, Wilts BA14 8RB, UK, 2001.

[3] Universal Metal finishing guidebook, Published by Metal finishing magazine, 2012-2013.

[4] S. M. Cohen, Review, Replacements for Chromium Pretreatments on Aluminum, *Corrosion* **51** (1), 71-78 (1995). DOI: <https://doi.org/10.5006/1.3293580>

[5] S. Lin, H. Shih, F. Mansfeld, Corrosion protection of aluminum alloys and metal matrix composites by polymer coatings, *Corrosion Science* **33** (9), 1331-1349 (1992). DOI: [https://doi.org/10.1016/0010-938X\(92\)90176-4](https://doi.org/10.1016/0010-938X(92)90176-4)

[6] J. Zhao, L. Xia, A. Sehgal, D. Lu, R.L. McCreery, G.S. Frankel, Effects of Chromate and Chromate Conversion Coatings on Corrosion of Aluminum Alloy 2024-T3. *Surf. Coat. Technol.* **140** (1), 51-57 (2001). DOI: [https://doi.org/10.1016/S0257-8972\(01\)01003-9](https://doi.org/10.1016/S0257-8972(01)01003-9)

[7] L. Xia, E. Akiyama, G. Frankel, R. McCreery, Storage and Release of Soluble Hexavalent Chromium from Chromate Conversion Coatings Equilibrium Aspects of  $\text{Cr}^{\text{VI}}$  Concentration. *J. Electrochem. Soc.* **147** (7), 2556-2562 (2000). DOI: <https://doi.org/10.1149/1.1393568>

[8] J. Zhao, G. Frankel, R.L. McCreery, Corrosion protection of untreated AA-2024-T3 in chloride solution by a chromate conversion coating monitored with Raman spectroscopy. *J. Electrochem. Soc.* **145** (7), 2258-2264 (1998). DOI: <https://doi.org/10.1149/1.1838630>

[9] J.F. Ying, M.Y. Zhou, B.J. Flinn, P.C. Wong, K.A.R. Mitchell, T. Foster, The effect of Ti-colloid surface conditioning on the phosphating of 7075-T6 aluminium alloy. *J. Mater. Sci.* **31**, 565-571 (1996). DOI: <https://doi.org/10.1007/bf00367870>

[10] M. Dabala, L. Armelao, A. Buchberger, I. Calliari, Cerium-based conversion layers on aluminum alloys. *Appl. Surf. Sci.* **172** (3-4), 312-322 (2001). DOI: [https://doi.org/10.1016/S0169-4332\(00\)00873-4](https://doi.org/10.1016/S0169-4332(00)00873-4)

[11] F. Deflorian, S. Rossi, L. Fedrizzi, Silane pre-treatments on copper and aluminium, *Electrochim. Acta* **51** (27), 6097-6103 (2006). DOI: <https://doi.org/10.1016/j.electacta.2006.02.042>

[12] M. Zhou, Q. Yang, T. Troczynski, Effect of substrate surface modification on alumina composite sol-gel coatings. *Surf. Coat. Technol.* **200** (8), 2800-2804 (2006). DOI: <https://doi.org/10.1016/j.surfcoat.2005.03.045>

[13] S. V. Kozhukharov, O. Acuna, M. Machkova, V. Kozhukharov, Influence of buffering on the spontaneous deposition of cerium conversion coatings for corrosion protection of AA2024-T3 aluminum alloy. *J. Appl. Electrochem.* **44** (10), 1093-1105 (2014). DOI: <https://doi.org/10.1007/s10800-014-0718-7>

[14] J.W. Bibber, A Chromium-Free Conversion Coatings for Aluminum. *Met. Finish.* **91** (12), 46-47 (1993).

[15] V. Ivanova, Y. Trifonova, P. Petkov, T. Petkova, The influence of In on photo-induced properties of Ge-Te-In chalcogenide thin films. *Optoelectronics and Advanced Materials – Rapid Communications* **8**, (1-2), 42-44 (2014).

- [16] Vl. Ivanova, Y. Trifonova, P. Petkov, Stress investigation in Ge-Te-In thin films. *Journal of Optoelectronics and Advanced Materials* **22** (5-6), 266-271 (2020).
- [17] V. Burokas, A. Martushene, A. Ruchinskene, A. Sudavichyus, G. Bikul'chyus, Deposition of amorphous phosphate coatings on aluminum. *Prot. Met.* **42**, 339-344 (2006).  
DOI: <https://doi.org/10.1134/S0033173206040059>
- [18] V. Burokas, A. Martušienė, O. Girčienė, Influence of fluoride ions on the amorphous phosphating of aluminium alloys. *Surf. Coat. Technol.* **202** (2), 239-245 (2007).  
DOI: <https://doi.org/10.1016/j.surfcoat.2007.05.034>
- [19] G. Ilieva, D. Ivanova, L. Fachikov, Thin phosphate films on aluminum surfaces. *Bulg. Chem. Commun.* **50** (special issue A), 55-60 (2018).
- [20] S.V. Kozhukharov, Ch. A. Girginov, Chapter 1: Classical and Modern Methods for Corrosion Impact Rate Determination for Aluminium and Strengthened Aircraft Alloys. *Fundamentals and Practical Applications*. Published in: *Phenomena and Theories in Corrosion Science. Methods of Prevention*, András Gergely Ed. NOVA Sci. Publ. (2019), p. 3-150; ISBN: 978-1-53615-252-4
- [21] B. Shri Prakash, J.N. Balaraju, Chromate (Cr6+)-free surface treatments for active corrosion protection of aluminum alloys: a review. *J. Coat. Technol. Res.* **21**, 105-135 (2024).  
DOI: <https://doi.org/10.1007/s11998-023-00831-1>
- [22] He Zhu, Jingfei Li, Advancements in corrosion protection for aerospace aluminum alloys through surface treatment, *International Journal of Electrochemical Science* **19** (2), 100487 (2024).  
DOI: <https://doi.org/10.1016/j.ijoes.2024.100487>
- [23] Adel Heydarian, Abolhassan Najafi, Gholamreza Khalaj, Enhancement of low-zinc phosphate coatings with addition Ni<sup>2+</sup> and Mn<sup>2+</sup> cations: Structure, corrosion resistance and paint adhesion. *Journal of Materials Research and Technolog* **30**, 7308-7327 (2024).  
DOI: <https://doi.org/10.1016/j.jmrt.2024.05.103>